Adaptive Pole Assignment Control for Generic Elastic Hypersonic Vehicle

Yan Binbin
The College of Astronautics, Northwestern Polytechnical University, Xi'an, Shanxi, China
Email: yanbinbin@ nwpu.edu.cn

***Abstract*—This paper uses robust pole assignment method to design an adaptive velocity and altitude tracking control algorithm for the longitudinal model of a wave rider configuration air-breathing hypersonic vehicle, which has strong coupling between structure, propulsion and aerodynamics. Base on the elastic hypersonic vehicle model CSUAL_GHV, the simulations using adaptive robust pole assignment control method and adaptive non-robust pole assignment control method are carried out respectively. The results show that, compared with the non-robust pole assignment control method, control system using adaptive robust pole assignment control method not only achieves the velocity and altitude tracking goal with tracking error less than 1%, but also the vibration motion of the hypersonic vehicle is suppressed sufficiently.**

***Index Terms*—hypersonic vehicle; elastic model; robust pole assignment; parameter identification; adaptive control**

I. Introduction

Air-breathing hypersonic vehicle is a kind of aircraft flying in the near space atmosphere, which is powered by scramjet and flying faster than 5 Mach. Because of its high speed, the hypersonic vehicle can be used as a military rapid combat platform as well as a fast civilian global transportation, and thus have received much attention. The last successful flight test of the U.S. X-51A "Waverider" hypersonic vehicle indicates that the hypersonic flight technology has been developed gradually from the experimental stage to the practical stage. Due to the use of airframe/engine integration design technology, the hypersonic vehicle exhibits strong coupling between structural, propulsion and aerodynamics. The hypersonic vehicle with waverider configuration is easy to generate elastic deformation because of the thin fore and aft. body. These characteristics pose a serious challenge to the design of hypersonic vehicle control system as in [1]. Based on this kind of hypersonic vehicle, we design an adaptive robust controller to realize the tracking of velocity and altitude command for the hypersonic vehicle at the present of elastic coupling.

For the modeling problem of the elastic hypersonic vehicle, Andrew D. Clark and Jason T. Parker *et al*. obtain a longitudinal motion model for control and simulation in [2], [3], Richard Colgren *et al.* gives an air-breathing hypersonic vehicle's longitudinal and lateral nonlinear equations of motion based on wind tunnel and computational fluid dynamics analysis in [4]. Michael A. Bolender *et al*. established the longitudinal motion equations of a hypersonic vehicle, deducted in detail the combustion characteristics of the scramjet which is integrated with the airframe, and obtained the mathematic model of the scramjet, and solved the elastic vibration motion of the vehicle using the Lagrange equation method in [5]. The hypersonic vehicle model named CSUAL_GHV is provided by Andrew D. Clark *et al*. According to their paper, the FLUENT CFD simulation technology is used to derive the aerodynamic data of the vehicle and the thrust data of the engine, and the NASTRAN program is used to solve the structure modes of the vehicle. Compared with the elastic model provided by Jason T. Parker, the CSUAL_GHV model treats the gravity acceleration as the function of altitude and takes the centrifugal inertial force into account. Considering the large flight envelope of the hypersonic vehicle, here we choose the CSUAL_GHV model as the hypersonic vehicle model for control system design and simulation analysis.

For the traditional configuration aircraft, the classical robust control technologies were shown to be effective to design perfect tracking controllers as in [6]-[9]. However, for hypersonic vehicle which has a large model uncertainty, classical robust control technology will be ineligible. As a kind of intelligent control technology, multivariable adaptive robust control technology is able to identify the vehicle's dynamic characteristics online, and adjust the parameters of the controller in real-time to achieve satisfactory control effect as in [10], [11]. Lisa Fiorentini *et al.* used a nonlinear sequential loop-closure approach to design a dynamic state-feedback controller that provides stable tracking of velocity and altitude reference trajectories in [12], [13]. Haojian Xu *et al.*, designed and realized the velocity and altitude reference command tracking control for the hypersonic vehicle using the neural network based MIMO robust adaptive control technology in [14]. In [15] the uncertainty modeling is implemented and a fixed order μ controller is designed for the hypersonic vehicle, and the comparison of control effects between full order and reduced order controllers was carried out. An adaptive linear quadratic controller based

Manuscript received October 10, 2013; revised November 11, 2013.

doi: 10.12720/joace.2.3.294-301

on the hypersonic vehicle model CSUAL_GHV is designed by Matthew Kuipers *et al.* and good control effect is achieved. But this approach requires that the idea reference model of the system is given, which is difficult for high order systems. Considering the above control strategies, this paper proposes the using of pole assignment method to design the adaptive control system. Considering the traditional state-feedback pole assignment method request the system to be completely controllable, while aircraft model obtained by online identification may not meet this requirement, a multivariable robust pole assignment approach is adopted.

II. Model of the Elastic Hypersonic Vehicle

The structure configuration of the hypersonic vehicle is illustrated in Fig. 1. The configuration of the vehicle used the body/engine integration design technology, which is the typical structure shape of waverider, as in [2].

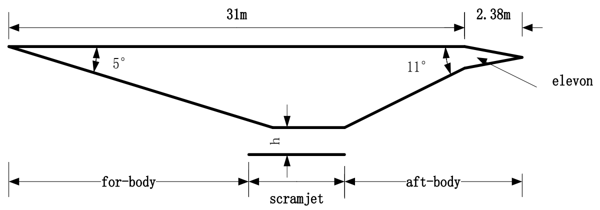

Figure 1. Geometry of the hypersonic vehicle.

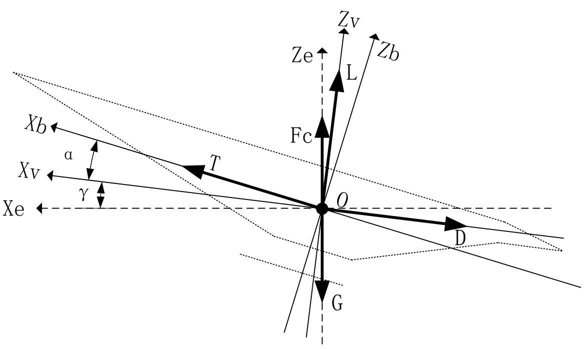

Figure 2. Longitudinal forces analysis of hypersonic vehicle.

Fig. 2 shows the forces and angles necessary to describe the longitudinal motion of the hypersonic vehicle. T, L and D are the external forces due to the aerodynamics and propulsion, $F_c = mV^2$ and $G = \mu m / r^2$ are centrifugal inertia force and gravity respectively, m is the vehicle mass, μ is the gravitational constant, $r = h + R_E$ is the distance between the center of mass of the vehicle and the center of earth, while the h and R_E are defined as the flight altitude and the earth's radius respectively, the vehicle velocity is represented by V, α and γ are the angle of attack and flight path angle.

According to the forces analysis show in Fig. 2, the longitudinal motion equation of the rigid hypersonic vehicle is obtained as bellow.

$$\begin{cases} \dot{V} = \dfrac{T\cos\alpha_r - D}{m} - \dfrac{\mu \sin\gamma}{r^2} \\ \dot{\gamma} = \dfrac{L + T\sin\alpha_r}{mV} - \dfrac{(\mu - V^2 r)\cos\gamma}{Vr^2} \\ \dot{h} = V\sin\gamma \\ \dot{\alpha}_r = q - \dot{\gamma} \\ \dot{q} = \dfrac{M_y}{I_y} \end{cases} \tag{1}$$

Here, I_y is the moment of inertia about the body y-axis and q is the pitch rate. The forces and moments are defined as follow,

$$\begin{cases} L = \frac{1}{2}\rho V^2 S \times C_L\left(Ma, \alpha, \delta_{e,r}, \delta_T\right) \\ D = \frac{1}{2}\rho V^2 S \times C_D\left(Ma, \alpha, \delta_{e,r}, \delta_T\right) \\ T = \frac{1}{2}\rho V^2 S \times C_T\left(Ma, \alpha, \delta_{e,r}, \delta_T\right) \\ M_y = \frac{1}{2}\rho V^2 S\overline{c} \times C_M\left(Ma, \alpha, \delta_{e,r}, \delta_T\right) \end{cases} \tag{2}$$

where ρ is the air density, S is the reference area, $\overline{c}$ is the mean aerodynamic chord, δ_T is throttle setting, Ma is the Mach number and $\delta_{e,r}$ is the rigid elevon deflection.

Due to the use of airframe/engine integration design technology, the hypersonic vehicle shows strong coupling characteristics among the structure, propulsion and aerodynamics. For the waverider configuration aircraft, the coupling characteristics appear more serious. By approximating the aircraft to a long thin plate, we can obtain the first three order bending mode of the flexible body using the Euler-Bernoulli beam theory.

$$\ddot{\eta}_i = -2\varsigma_i \omega_i \dot{\eta}_i - \omega_i^2 \eta_i + P / M_i \quad i = 1,2,3 \tag{3}$$

Here, η_i is the i^{th} elastic generalized coordinate, ω_i and ς_i are the frequency and the damping ratio of i^{th} elastic modal respectively, P is the normal force at the elevon hinge produced by the elevon, and M_i is the i^{th} modal generalized mass. It is assume that the elastic deformation of the vehicle will only affect the angle of attack and the deflection of elevon, that's to say the effective angle of attack α and deflection of elevon δ_e are consisted of rigid and elastic part.

$$\begin{cases} \alpha = \alpha_r + \alpha_e = \alpha_r + \sum\limits_{i=1}^{3} \tau_{n,i}\eta_i \\ \delta_e = \delta_{e,r} + \delta_{e,e} = \delta_{e,r} + \sum\limits_{i=1}^{3} \tau_{t,i}\eta_i \end{cases} \tag{4}$$

where α_r and α_e are the rigid and elastic angle of attack respectively, the constant $\tau_{t,i}$ scales the generalized elastic coordinate to elastic elevon deflection, and $\tau_{n,i}$ is the nose coordinate scaling factor.

Finally, the equation (1), (3) and (4)together make up the longitudinal motion equations of the elastic hypersonic vehicle.

III. Description of the Control System

Due to the use of airframe/engine integration design technology, the vehicle will suffer great aerodynamic force and moment under the condition of high Mach number and maneuvering flight in large range. As a result, the vehicle's airframe will generate elastic vibration, which will change the aerodynamic characteristics of the vehicle, and in turn affects the control effect of the control system.

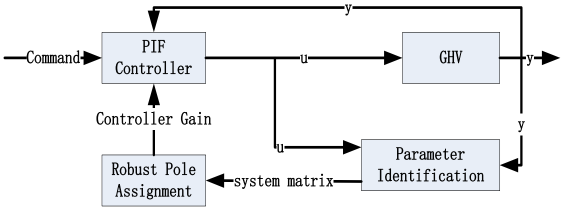

Figure 3. Control system diagram.

In view of the hypersonic vehicle model uncertainty and the body elastic deformation characteristics, the adaptive control algorithm is adopted. According to the adaptive control algorithm, the dynamic characteristics of the hypersonic vehicle are obtained through online parameter identification, and the robust pole assignment approach is employed to design the velocity and altitude tracking control system. By such method, the suppression of the elastic vibration and good dynamic quality of the hypersonic vehicle is expected.

The control system diagram using adaptive robust pole assignment algorithm is illustrated in Fig. 3.

It can be seen from the diagram that, the control system is mainly consist with four parts, which is aircraft model, parameter identification, pole assignment and PIF controller. The aircraft model describes the longitudinal motion of the hypersonic vehicle, while the parameter identification block identifies the linear state-space model of the vehicle using the input and output signals of the aircraft model, and then the linear state-space model is used by the robust pole assignment algorithm to design the PIF command tracking controller.

IV. Controller Design

In the process of controller design for the elastic hypersonic vehicle, the elastic deformation effects on the angle of attack and deflection of elevon are treated as disturbances. The robust controller is designed for the rigid motion of the vehicle, which is able to suppress the elastic deformation disturbance of the hypersonic vehicle. To design the controller, the following linear state-space equation for the longitudinal motion of the vehicle is considered.

$$\begin{cases} \triangle \dot{\boldsymbol{x}} = \boldsymbol{A}\triangle \boldsymbol{x} + \boldsymbol{B}\triangle \boldsymbol{u} \\ \triangle \boldsymbol{y} = \boldsymbol{C}\triangle \boldsymbol{x} \end{cases} \tag{5}$$

Here $\triangle \boldsymbol{x} = \left[\triangle V, \triangle\gamma, \triangle h, \triangle\alpha, \triangle q\right]^T$ is the state vector of the hypersonic vehicle, $\triangle \boldsymbol{u} = \left[\triangle\delta_{T,c}, \triangle\delta_{e,c}\right]^T$ is the control vector, $\triangle\delta_{T,c}$ and $\triangle\delta_{e,c}$ is the throttle setting and elevon deflection command respectively, $\boldsymbol{B}$ is a matrix with full column rank, $\triangle \boldsymbol{y} = \triangle \boldsymbol{x}$ is the measurable output vector of the vehicle which means that the state vector can be measured from the vehicle's outputs. To achieve the goal of velocity and altitude command tracking control, the index vector is defined as follow.

$$\triangle \boldsymbol{z} = \left[\triangle V, \triangle h\right]^T = \boldsymbol{H}\triangle \boldsymbol{x} \tag{6}$$

The following matrix equation should be satisfied when the steady state reached:

$$\begin{bmatrix} 0 \\ \triangle \boldsymbol{z}^* \end{bmatrix} = \begin{bmatrix} \boldsymbol{A} & \boldsymbol{B} \\ \boldsymbol{H} & 0 \end{bmatrix} \begin{bmatrix} \triangle \boldsymbol{x}^* \\ \triangle \boldsymbol{u}^* \end{bmatrix} \tag{7}$$

Here, $\triangle \boldsymbol{z}^*$ is the desired index vector, $\triangle \boldsymbol{x}^*$ and $\triangle \boldsymbol{u}^*$ are the steady state vector and steady control vector.

Define the matrix:

$$\boldsymbol{G} = \begin{bmatrix} \boldsymbol{A} & \boldsymbol{B} \\ \boldsymbol{H} & \boldsymbol{0} \end{bmatrix}^{-1} = \begin{bmatrix} \boldsymbol{G_{11}} & \boldsymbol{G_{12}} \\ \boldsymbol{G_{21}} & \boldsymbol{G_{22}} \end{bmatrix} \tag{8}$$

Then, from equation (7) and (8) the following equation can be satisfied,

$$\begin{bmatrix} \triangle \boldsymbol{x}^* \\ \triangle \boldsymbol{u}^* \end{bmatrix} = \begin{bmatrix} \boldsymbol{G_{12}} \\ \boldsymbol{G_{22}} \end{bmatrix} \triangle \boldsymbol{z}^* \tag{9}$$

The purpose of the controller is to track the command velocity and altitude, which means that the following equation must be satisfied,

$$\lim_{t\to t_1} \triangle \boldsymbol{e}(t) = \lim_{t\to t_1} (\triangle \boldsymbol{z}(t) - \triangle \boldsymbol{z}^*(t)) = \boldsymbol{0} \tag{10}$$

Combining the equation (9) and (10) obtains

$$\begin{aligned} &\lim_{t\to t_1} \begin{bmatrix} \triangle \boldsymbol{x}(t) - \triangle \boldsymbol{x}^*(t) \\ \triangle \boldsymbol{u}(t) - \triangle \boldsymbol{u}^*(t) \end{bmatrix} \\ &= \begin{bmatrix} \boldsymbol{G_{12}} \\ \boldsymbol{G_{22}} \end{bmatrix} \lim_{t\to t_1} \left(\triangle \boldsymbol{z}(t) - \triangle \boldsymbol{z}^*(t) \right) = \boldsymbol{0} \end{aligned} \tag{11}$$

Defining the error vector as follow,

$$\begin{bmatrix} \triangle \tilde{\boldsymbol{x}}(t) \\ \triangle \tilde{\boldsymbol{u}}(t) \end{bmatrix} = \begin{bmatrix} \triangle \boldsymbol{x}(t) - \triangle \boldsymbol{x}^*(t) \\ \triangle \boldsymbol{u}(t) - \triangle \boldsymbol{u}^*(t) \end{bmatrix} \tag{12}$$

Then the task of the controller design is to design the control algorithm that makes the error vector converges to zero in finite time, that's

$$\lim_{t\to t_1} \begin{bmatrix} \triangle \tilde{\boldsymbol{x}}(t) \\ \triangle \tilde{\boldsymbol{u}}(t) \end{bmatrix} = \boldsymbol{0} \tag{13}$$

To achieve zero steady-state error to constant commands, integral action is added by augmenting the state vector with the integral of the error

$$\triangle \boldsymbol{e_I}(t) = \int_{t_0}^{t_1} \triangle \boldsymbol{e}(\tau) d\tau = \int_{t_0}^{t_1} \boldsymbol{H} \triangle \tilde{x}(\tau) d\tau \tag{14}$$

here $\triangle \boldsymbol{e}(t) \triangleq \triangle \boldsymbol{z}(t) - \triangle \boldsymbol{z}^*(t) = \boldsymbol{H} \triangle \tilde{x}(t)$.

As mentioned before, the elastic deformation of the vehicle is treated as disturbances to the angle of attack and deflection of elevon, to suppress the disturbances, the band width of control signal must be limited, as in [16]. This can be achieved by appending low-pass filter to the controller, that's to say $\triangle \boldsymbol{v} = \triangle \dot{\tilde{\boldsymbol{u}}}$ and let the $\triangle \boldsymbol{v}$ as the new input signal. Considering $\triangle \tilde{\boldsymbol{u}} = \triangle \boldsymbol{u} - \triangle \boldsymbol{u}^*$, which means that filtering $\triangle \tilde{\boldsymbol{u}}$ is filtering $\triangle \boldsymbol{u}$.

Based on the above analysis, the augmented system can be obtained as follow

$$\begin{bmatrix} \triangle \dot{\tilde{\boldsymbol{x}}} \\ \triangle \dot{\boldsymbol{e}}_{\boldsymbol{I}} \\ \triangle \dot{\tilde{\boldsymbol{u}}} \end{bmatrix} = \begin{bmatrix} \boldsymbol{A} & \boldsymbol{0} & \boldsymbol{B} \\ \boldsymbol{H} & \boldsymbol{0} & \boldsymbol{0} \\ \boldsymbol{0} & \boldsymbol{0} & \boldsymbol{0} \end{bmatrix} \begin{bmatrix} \triangle \tilde{\boldsymbol{x}} \\ \triangle \boldsymbol{e_I} \\ \triangle \tilde{\boldsymbol{u}} \end{bmatrix} + \begin{bmatrix} \boldsymbol{0} \\ \boldsymbol{0} \\ \boldsymbol{I} \end{bmatrix} \triangle \boldsymbol{v} \tag{15}$$

Defining the error vector $\boldsymbol{e} = \begin{bmatrix} \triangle \tilde{x} & \triangle \boldsymbol{e_I} & \triangle \tilde{\boldsymbol{u}} \end{bmatrix}^T$, then equation (15) can be expressed in the state-space form

$$\dot{\boldsymbol{e}} = \boldsymbol{A_e} \boldsymbol{e} + \boldsymbol{B_e} \triangle \boldsymbol{v} \tag{16}$$

where,

$$\boldsymbol{A_e} = \begin{bmatrix} \boldsymbol{A} & \boldsymbol{0} & \boldsymbol{B} \\ \boldsymbol{H} & \boldsymbol{0} & \boldsymbol{0} \\ \boldsymbol{0} & \boldsymbol{0} & \boldsymbol{0} \end{bmatrix}, \boldsymbol{B_e} = \begin{bmatrix} \boldsymbol{0} \\ \boldsymbol{0} \\ \boldsymbol{I} \end{bmatrix}$$

Assuming that the linear system (16) is controllable completely, then the system can be stabilized by state feedback pole assignment, as in [17]. Let the state feedback control law to be $\triangle \boldsymbol{v} = -\boldsymbol{Ke}$, substituting into the equation (16) obtains

$$\dot{\boldsymbol{e}} = \left(\boldsymbol{A_e} - \boldsymbol{B_e} \boldsymbol{K}\right) \boldsymbol{e} \tag{17}$$

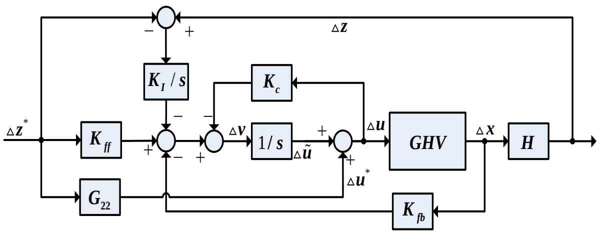

Figure 4. Control system diagram of the hypersonic vehicle.

By appropriately select the closed-loop poles of the system, the error vector $\boldsymbol{e}$ will converge to zero exponentially.

According to the state feedback control law $\triangle \boldsymbol{v} = -\boldsymbol{Ke}$, we have

$$\begin{aligned} \triangle \boldsymbol{v} &= -\begin{bmatrix} \boldsymbol{K_1} & \boldsymbol{K_2} & \boldsymbol{K_3} \end{bmatrix} \begin{bmatrix} \triangle \tilde{\boldsymbol{x}} \\ \triangle \boldsymbol{e_I} \\ \triangle \tilde{\boldsymbol{u}} \end{bmatrix} \\ &= \left(\boldsymbol{K_1 G_{12}} + \boldsymbol{K_3 G_{22}}\right) \triangle \boldsymbol{z}^* - \boldsymbol{K_1} \triangle \boldsymbol{x} - \boldsymbol{K_2} \triangle \boldsymbol{e_I} - \boldsymbol{K_3} \triangle \boldsymbol{u} \\ &= \boldsymbol{K_{ff}} \triangle \boldsymbol{z}^* - \boldsymbol{K_{fb}} \triangle \boldsymbol{x} - \boldsymbol{K_I} \triangle \boldsymbol{e_I} - \boldsymbol{K_c} \left(\triangle \tilde{\boldsymbol{u}} + \triangle \boldsymbol{u}^*\right) \end{aligned}$$

where $\boldsymbol{K_{ff}} = \boldsymbol{K_1 G_{12}} + \boldsymbol{K_3 G_{22}}$, $\boldsymbol{K_{fb}} = \boldsymbol{K_1}$, $\boldsymbol{K_I} = \boldsymbol{K_2}$ and $\boldsymbol{K_c} = \boldsymbol{K_3}$.

According to equation (1), the controller structure of the hypersonic vehicle is illustrated as Fig. 4, which is the so called proportion-integration-filter(PIF) controller in [18].

V. Robust Pole Assignment

In the previous controller design section, the state feedback pole assignment algorithm is used to compute the controller gain and stabilize the system. But the classical state feedback pole assignment algorithm requires that the system must be controllable completely, which is usually unsatisfied. To this end, J. Kautsky put forward the linear state feedback robust pole assignment algorithm in [19], which does not require the system to be completely controllable and at the same time lowers the sensitive of the poles to the system disturbances, equips the system with good robustness.

Considering the MIMO linear time-invariant state-space function,

$$\dot{\boldsymbol{x}} = \boldsymbol{Ax} + \boldsymbol{Bu} \tag{19}$$

Here, $\boldsymbol{B}$ is a matrix with full column rank. Assuming that the desired closed-loop poles are $\lambda_i, i = 1, 2, ..., n$, then the robust pole assignment is to determine the real matrix $\boldsymbol{K}$ and the non-singular matrix that satisfy the following equation

$$\left(\boldsymbol{A} - \boldsymbol{BK}\right) \boldsymbol{X} = \boldsymbol{X\Lambda} \tag{20}$$

where, the diagonal matrix $\boldsymbol{\Lambda} = diag([\lambda_1, \lambda_2, ..., \lambda_n])$, the nonsingular matrix $\boldsymbol{X} = \left[\boldsymbol{x_1}, \boldsymbol{x_2}, ..., \boldsymbol{x_n}\right]$, and $\boldsymbol{x_i}$ is the eigenvector corresponding to the eigenvalue λ_i.

The necessary and sufficient condition for the existence of solution $\boldsymbol{K}$ in equation (20) is [14]

$$\boldsymbol{U}_1^T \left(\boldsymbol{AX} - \boldsymbol{X\Lambda}\right) = \boldsymbol{0} \tag{21}$$

and the solution is

$$\boldsymbol{K} = \boldsymbol{Z}^{-1} \boldsymbol{U}_0^T \left(\boldsymbol{A} - \boldsymbol{X\Lambda X}^{-1}\right) \tag{22}$$

Considering that the matrix $\boldsymbol{B}$ is full column rank, it can be resolved as

$$\boldsymbol{B} = \begin{bmatrix} \boldsymbol{U}_0 & \boldsymbol{U}_1 \end{bmatrix} \begin{bmatrix} \boldsymbol{Z} \\ \boldsymbol{0} \end{bmatrix} \tag{23}$$

$\boldsymbol{U} = \begin{bmatrix} \boldsymbol{U}_0 & \boldsymbol{U}_1 \end{bmatrix}$ is the orthogonal matrix and $\boldsymbol{Z}$ is the nonsingular matrix.

Assuming the state feedback gain $\boldsymbol{K}$ place the closed-loop poles to the stable poles $\lambda_i, i = 1, 2, ..., n$, then the matrix of perturbed closed-loop system $\boldsymbol{A} - \boldsymbol{BK} + \boldsymbol{\Delta}$ remains stable for all perturbations $\boldsymbol{\Delta}$ satisfying the following condition.

For the continuous time system, the condition is

$$\|\boldsymbol{\Delta}\|_2 < \min_{s=i\omega} \sigma_n \left\{s\boldsymbol{I} - (\boldsymbol{A} - \boldsymbol{BK})\right\} \triangleq \delta(\boldsymbol{K}) \tag{24}$$

and the lower bound of $\delta(\boldsymbol{K})$ is determined by the following inequality

$$\delta(\boldsymbol{K}) \ge \min_j \mathrm{Re}(-\lambda_j) / \kappa_2(\boldsymbol{X}) \tag{25}$$

Here, $\kappa_2(\boldsymbol{X})$ is the condition number of the eigenvector matrix $\boldsymbol{X}$.

For the discrete time system,

$$\|\boldsymbol{\Delta}\|_2 < \min_{s=\exp(i\omega)} \sigma_n \left\{ s\boldsymbol{I} - (\boldsymbol{A} - \boldsymbol{BK}) \right\} \equiv \delta(\boldsymbol{K}) \tag{26}$$

where the $\delta(\boldsymbol{K})$ satisfies

$$\delta(\boldsymbol{K}) \ge \min_j (1 - |\lambda_j|) / \kappa_2(\boldsymbol{X}) \tag{27}$$

From the equations (24), (25), (26) and (27) we can infer that under the condition provide by equation (20), the eigenvector matrix $\boldsymbol{X}$ is adjusted according to its condition number. The smaller the condition number the better robustness for the system.

To compute the eigenvector matrix $\boldsymbol{X}$ which satisfies the above conditions, J. Kautsky *et al*. provide four numeric iterative algorithms in [19], and compare the condition numbers computed by the four algorithms.

VI. Model Identification

The controller design and analysis for the hypersonic vehicle in previous sections is based on the linear model of the hypersonic vehicle, which is obtained by small disturbance linearization method at the trim point. But, due to the large velocity and altitude range of the hypersonic vehicle, the controller design for some trim points is not sufficient for the whole flying envelope. So we need to introduce some mechanism to compute the linearized model of the hypersonic vehicle and adjust the controller gain accordingly to get the satisfactory control effects.

To identify the controlled system online, the parameterized model of the controlled system must be determined firstly. Given the linear state-space model of the hypersonic vehicle as bellow

$$\begin{cases} \triangle \dot{\boldsymbol{x}} = \boldsymbol{A} \triangle \boldsymbol{x} + \boldsymbol{B} \triangle \boldsymbol{u} \\ \triangle \boldsymbol{y} = \boldsymbol{C} \triangle \boldsymbol{x} \end{cases} \tag{28}$$

where, $\triangle \boldsymbol{x} = [\triangle V, \triangle \gamma, \triangle h, \triangle \alpha, \triangle q]^T$ is the state vector, $\triangle \boldsymbol{u} = \left[\triangle \delta_{T,c}, \triangle \delta_{e,c}\right]^T$ is the control vector, the output matrix $\boldsymbol{C} = \boldsymbol{I}_{5\times5}$, which means that the state vector of the system can be measured through the system outputs. The i^{th} state derivative can be expressed as

$$\triangle \dot{x}_i = \sum_{j=1}^{5} a_{ij} \triangle x_j + \sum_{j=1}^{2} b_{ij} \triangle u_j + \varepsilon_i \tag{29}$$

ε_i is the measurement noise.

Defining the parameter vector $\boldsymbol{\theta_i} = [a_{i1}, a_{i2}, ..., a_{i5}, b_{i1}, b_{i2}]^T$ and the regressive vector $\phi = \left[\triangle V, ..., \triangle q, \triangle \delta_{T,c}, \triangle \delta_{e,c}\right]^T$, ignoring the noise item ε_i in equation (29) obtains

$$\triangle \dot{\boldsymbol{x}}_{\boldsymbol{i}} = \boldsymbol{\theta}_{\boldsymbol{i}}^T \phi \quad i = 1, 2, ..., 5 \tag{30}$$

Equation (30) is the parameterized model of the system (28).

According to the linear system (28), the regressive vector ϕ is measurable, while the state derivatives is usually immeasurable. Thus, we need to filter the state vector to get the state derivatives. That is to say, by taking the Laplace transform to equation (30) and multiplying $1/\Lambda(s)$ to both sides, the new linear parameterized model can be obtained as bellow.

$$z_i = \frac{s}{\Lambda(s)} \triangle x_i(s) = \frac{1}{\Lambda(s)} \boldsymbol{\theta}_{\boldsymbol{i}}^T \phi = \boldsymbol{\theta}_{\boldsymbol{i}}^T \overline{\phi} \tag{31}$$

Here $\Lambda(s) = s + \lambda$, λ is the design parameter and $\overline{\phi} = \phi / \Lambda(s)$.

After the parameterized model is determined, we need an adaptive law to make the identified parameters converge to the true value as soon as possible. The commonly used parameter identification methods include the recursive least-square method with forgetting factor, the recursive gradient method, the maximum likelihood estimation method and recursive newton method as in [20]. The least-square method has high identification precision and convergent fast, but the amount of computations is too large. The precisions of the maximum likelihood method and the newton method are too low. The recursive gradient method is simple and convergent quickly. Here, we choose the recursive gradient method as the adaptive law to identify the system matrix $\boldsymbol{A}$ and $\boldsymbol{B}$. The recursive gradient method is listed bellow

$$\begin{aligned} \hat{\boldsymbol{\theta}}(k) &= \hat{\boldsymbol{\theta}}(k-1) \\ &+ \frac{\alpha \phi(k)}{c + \phi^T(k)\phi(k)} \left[y(k) - \hat{\boldsymbol{\theta}}^T(k-1)\phi(k) \right] \end{aligned} \tag{32}$$

here $0 < \alpha < 2, c > 0$ is the design parameter.

VII. Simulation

The simulation is based on the control oriented hypersonic vehicle model named CSUAL_GHV given by Andrew D. Clark *et al*. in [2]. The initial velocity and altitude of the vehicle is 10 Mach and 30 km. The trim states of the vehicle under the initial flight conditions and the poles of the system are listed in the Table I and Table II.

TABLE I. Trim Conditions of the Hypersonic Vehicle

State	Value
Velocity (m/s)	3026
Flight path angle (deg)	0
Altitude (m)	30000
Angle of attack (deg)	0.0822
Pitch rate (deg/s)	0
Elastic deformation of the for-body (deg)	0.1229
Elastic deformation of the aft- body (deg)	0.1816
Throttle setting	0.0630
Deflection of the elevon (deg)	-7.8850

It can be seen from Table II that the elastic motion of the hypersonic vehicle is stable while the rigid motion contains the positive pole, which is unstable. According to the methods described before, the system can be stabilized using the state feedback pole assignment method.

TABLE II. POLES OF THE HYPERSONIC VEHICLE

Rigid body poles	Elastic body poles
-0.00036	-0.20 ±20.6i
-5.27×10-6 ±0.03i	-0.59 ±58.8i
2.60	-1.16 ±116i
-2.72	

According to the analysis in the previous sections, the simulation model of the hypersonic vehicle is built under the Matlab/Simulink environment in [21]. The command speed and altitude increments are 300m/s and 3660m respectively, the command signal is filtered to make it smooth, the transfer function of the filter is

$$P(s) = \frac{0.05^2}{s^2 + 0.1s + 0.05^2} \tag{33}$$

The design parameters of the recursive gradient method are $\alpha = 0.001$ and $c = 1$, initial value for the identified matrices are chosen from the linearized model of the initial trim point, the desired closed-loop poles are

$$\lambda_m = -0.1, -0.5, -1, -2, -2-i, -2+i, -3, -4, -5$$

The simulation results are showed in figures 5~13 given in Appendix A. Fig. 5 plots the vehicle's velocity and altitude curves and the tracking error, it can be seen from the figure that the system can track the command signals rapidly with small tracking errors. Hence, the adaptive robust pole assignment control law is suitable for the velocity and altitude control of the hypersonic vehicle with strong aerodynamic/elastic coupling.

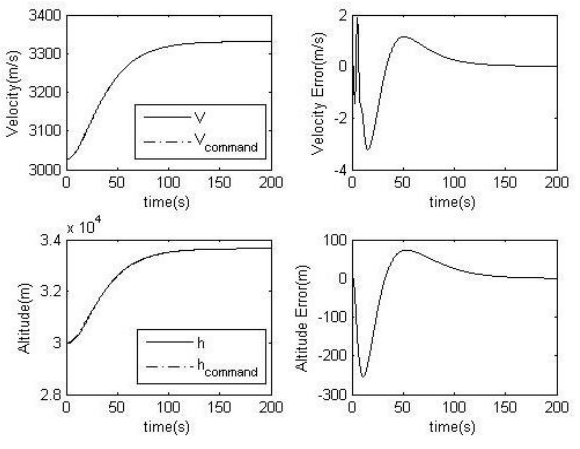

Figure 5. Velocity and altitude tracking output of the hypersonic vehicle.

The Fig. 6 and Fig. 7 show that during the speed up and climbing stage, the vehicle bears strong aerodynamic forces and moments, the structure deformation occurs and converges to constant value finally.

To compare the control effects of adaptive robust pole assignment method (M1) and adaptive non-robust pole assignment method (M2), the simulations of the two cases are carried out.

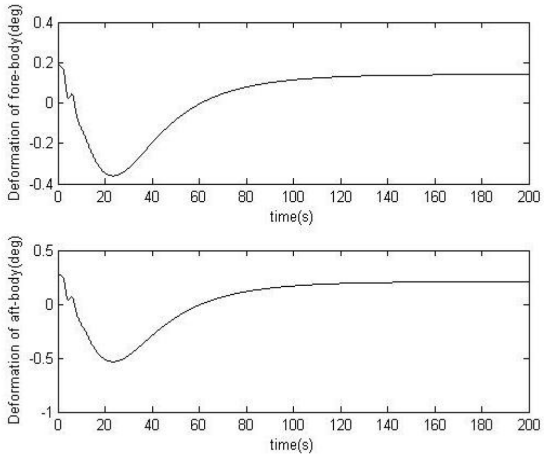

Figure 6. Elastic deformation of the fore-body and aft-body.

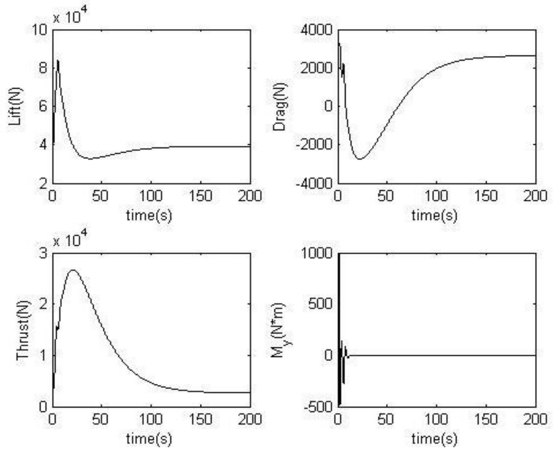

Figure 7. The forces and moments

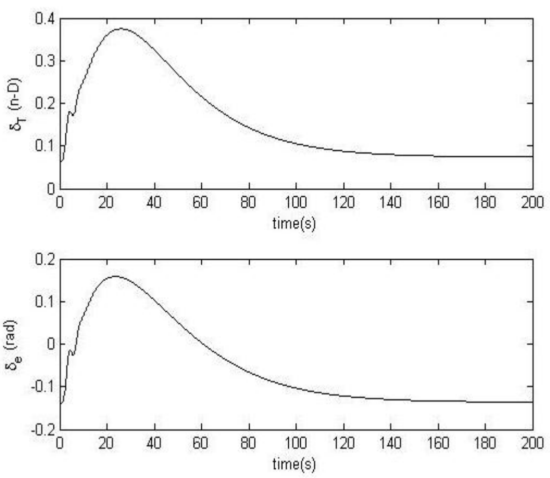

Figure 8. The controls with adaptive robust pole assignment control.

The control values of the vehicle using adaptive robust pole assignment method and adaptive non-robust pole assignment method are illustrated in Fig. 8 and Fig. 9. It can be seen from the figures that the control signal of the adaptive robust pole assignment method is smooth, while it's oscillating sharply due to the aerodynamic elastic vibration of the vehicle using the adaptive non-robust pole assignment method, which is unable to suppress the aerodynamic elastic vibration of the vehicle sufficiently.

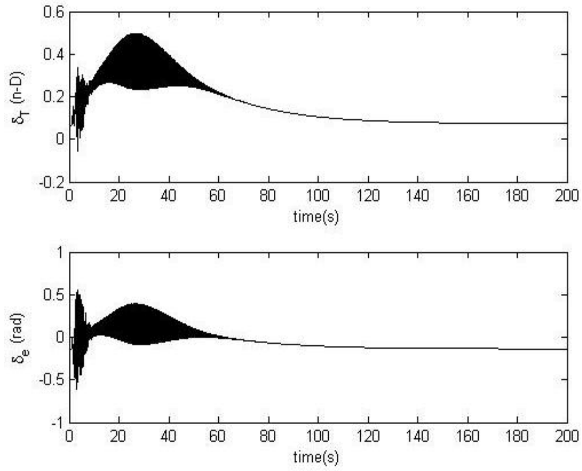

Figure 9. The controls with adaptive non-robust pole assignment control.

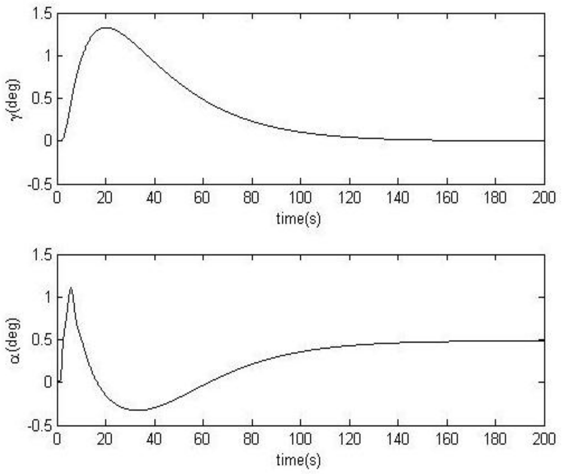

Figure 10. Flight path angle and angle of attack with adaptive robust pole assignment control.

For the hypersonic vehicle using the scramjet as the power, the angle of attack must be limited to a little value(±2°) for the proper work of the scramjet. Fig. 10 and Fig. 11 show the curves of flight path angle and angle of attack for two methods respectively. It can be concluded from the figures that the angle of attack of the vehicle using the M1 control method is less than and more smooth than the M2 case, which means that the M1 control method is more suitable for the control of an elastic vehicle.

The Fig. 12 and Fig. 13 illustrate the elastic motion of the vehicle in the two cases respectively. Comparing the two figures, we can reach the conclusion that the control system designed by the adaptive robust pole assignment method is able to suppress the elastic vibration of the vehicle and as a result equip the vehicle with good dynamic quality.

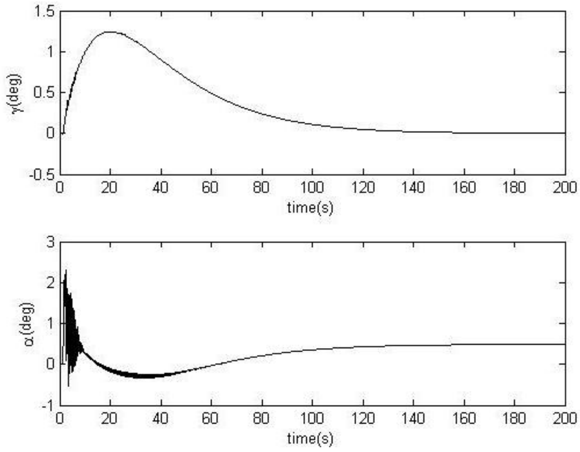

Figure 11. Flight path angle and angle of attack with adaptive non-robust pole assignment control.

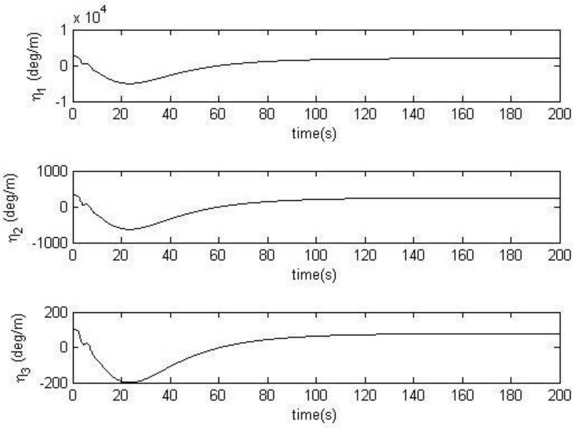

Figure 12. Elastic modal with adaptive robust pole assignment control.

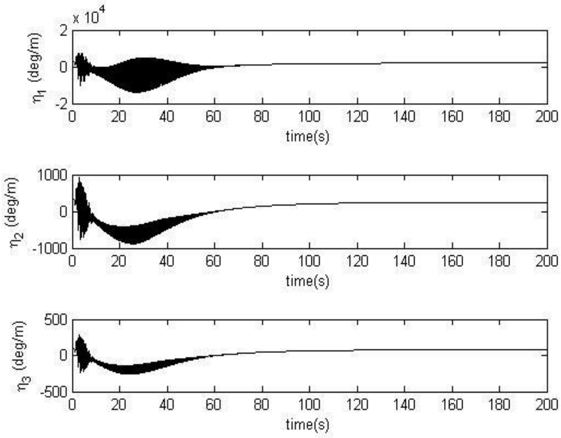

Figure 13 Elastic modal with adaptive non-robust pole assignment control.

VIII. Conclusion

From the simulation result and analysis in the previous sections, we can reach the conclusions as following.

1) Hypersonic vehicle using the waverider configuration is vulnerable to strong elastic

vibration during the maneuvering due to the special structure shape of the vehicle.

2) It is easy to realize the velocity and altitude tracking control by the adaptive control law, which is designed using the robust pole assignment method.
3) The controller designed using adaptive robust pole assignment control law is able to suppress the elastic motion of the hypersonic vehicle sufficiently.

ACKNOWLEDGMENT

This work was supported by the National Natural Science Foundation of China [grant numbers 61104195].

REFERENCES

[1] Y. H. Tang, S. L. Chen, and M. Xu, "The revolution of hyper-sonic technology and its aero-elasticity problem," *Flight Mechanics and Flight Test Academic Exchange Conference Papers*, 2004, pp. 10-15.

[2] A. D. Clark, M. D. Mirmirani, C. Wu *et al*., "An aero-propulsion integrated elastic model of a generic airbreathing hypersonic vehicle," in *Proc. AIAA Guidance, Navigation and Control Conference and Exhibit*, 2006, pp. 21-24.

[3] J. T. Parker, M. A. Bolender, and D. B. Doman, "Control-oriented modeling of an air-breathing hypersonic vehicle," *Journal of Guidance, Control and Dynamics*, vol. 30, pp. 856-869, 2007.

[4] R. Colgren, S. Keshmiri， and M. Mirmirani, "Nonlinear ten-degree-of-freedom dynamics model of a generic hypersonic vehicle," *Journal of Aircraft*, vol. 46, no. 3, 2009.

[5] M. A. Bolender and D. B. Doman, "A nonlinear model for the longitudinal dynamics of a hypersonic air-breathing vehicle," in *Air Force Research Laboratory*, Wright-Patterson AFB, OH 45433, 2006.

[6] C. I. Marrison and R. F. Stengel, "Design of robust control system for a hypersonic aircraft," *AIAA Journal of Guidance, Control, and Dynamics*, vol. 21, pp. 58-63, 1998.

[7] R. D. Colgren, *Non-linear h∞ Control of a Missile'S Roll Axis*, American Control Reference, 1994.

[8] R. J. Adams *et al.*, *Robust Multivariable Flight Control*, Springer-Verlag, 1994.

[9] P. Liu and L. X. Gu, "Optimal tracking control of a hypersonic vehicle using dynamic output feedback," *Journal of Harbin Institute of Technology*, 2011.

[10] P. A. Ioannou and J. Sun, *Robust Adaptive Control*, Upper Saddle River, NJ: Prentice-Hall, 1996.

[11] J. Sun and P. A. Ioannou, "Robust adaptive lq control schemes," *IEEE Transactions on Automatic Control*, vol. 37, pp. 100-106, 1992.

[12] L. Fiorentini, A. Serrani *et al.*, "Nonlinear ro-bust/adaptive controller design for an air-breathing hypersonic vehicle model," in *Proc. AIAA Guidance, Navigation and Control Conference and Exhibit*, 2007, pp. 20-23.

[13] L. Fiorentini, A. Serrani *et al*., "Nonlinear control of a hypersonic vehicle with structural flexibility," in *Proc. 47th IEEE Conference on Decision and Control Cancun*, Mexico, Dec 9-11, 2008.

[14] H. J. Xu, M. Mirmirani, and P. A. Ioannou, "Robust neural adaptive control of a hypersonic air-craft," in *Proc. AIAA Guidance, Navigation, and Control Conference and Exhibit*, 2003, pp. 11-14.

[15] H. Buschek and A. J. Calise, "Uncertainty modeling and fixed-order controller design for a hypersonic vehicle model," *Journal of Guidance, Control, and Dynamics*, vol. 20, no. 1, 1997.

[16] M. Kuipers, M. Mirmirani, P. Ioannou *et al.*, "Adaptive control of an aeroelastic airbreathing hypersonic cruise vehicle," in *Proc. AIAA Guidance, Navigation and Control Conference and Exhibit*, 2007, pp. 20-23.

[17] D. Z. Zheng, *Linear System Theory* (Second Edition), Beijing: Tsinghua University Press, 2002, pp. 258-285.

[18] R. F. Stengel, *Flight Dynamics*, Princeton, NJ: Princeton University Press, 2004, pp. 428-438.

[19] J. Kautsky, N. K. Nichols, and P. Van Dooren, "Robust pole assignment in linear state feedback," *International Journal of Control*, vol. 41, pp. 1129-1155, 1985.

[20] Z. H. Pang and H. Cui, *System Identification and Adaptive Control with MATLAB Simulation*, Beijing: Beijing University of Aeronautics and Astronautics Press, 2009, pp. 11-58.

[21] D. Y. Xue and Y. Q. Chen, *System Simulation Technology and Its Application Base on MATLAB/Simulink*, Beijing: Tsinghua University Press, 2002.

Binbin Yan received the M.Sc. degree and the Ph.D. degree in navigation, guidance and control, from the College of Astronautics of Northwestern Polytechnical University, China, in 2007 and 2010 respectively. From 2010 to 2013 he was a Postdoctor at the College of Astronautics of Northwestern Polytechnical University.He joined the College of Astronautics of Northwestern Polytechnical University, in 2010. He participated as a lecturer in the research program ''Flight control syetem design of the hypersonic vehicle'' .